

*Opinion paper***Porosity in minerals****Ekhard K.H. Salje***

Department of Earth Sciences, University of Cambridge, Cambridge CB2 3EQ, UK

* **Correspondence:** Email: ekhard@esc.cam.ac.uk.

Abstract: Minerals typically form porous assemblies with porosity extending from a few percent to ca. 35% in porous sandstones, and over 50% in tuff, clays, and tuff. While transport of gases and liquids are widely researched in these materials, much less is known about their mechanical behaviour under stress. With the development of artificial porous materials such questions become more pertinent, e.g., for applications as fillers in car bumpers and airplane wings, and nanoscale applications in memistors and neuromorphic computers. This article argues that elasticity and related dielectric and magnetic properties can be described-to some extent-as universal in porous materials. The collapse of porous materials under stress triggers in many cases avalanches of collapsed regions which are scale invariant and follow irreversible power law energy emission. Emphasis is given to a recent simple collapse model by Casals and Salje which covers many of the observed phenomena.

Keywords: porous minerals; avalanches; porous collapse; mechanical stability; ferroelasticity

1. Introduction

The importance of porosity as a mineral parameter outside fluid mechanics is often underrated. Still, there is hardly any other parameter which has such a massive effect on the physical and chemical properties of commonly used materials from mechanical stability to greatly increased “intrinsic” surfaces for catalytic applications. It is a parameter which matters greatly in geological sciences. The American Mineralogist, in a Centennial article, referred to “twins, tweed and holes” as indicators for minerals which are likely to be topics of enhance future research [1]. The term “holes” stands here for porosity. If we focus on the mechanical stability of minerals, we find that porosity changes the bulk

modulus in an approximately universal fashion when the measured elasticity is normalized with respect to the non-porous matrix (Figure 1, after [2])

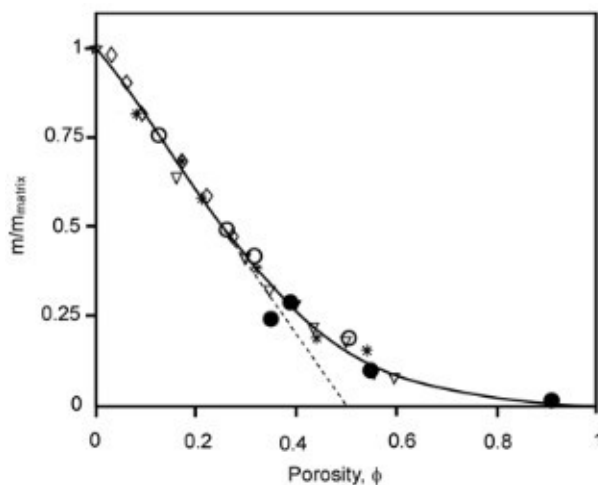


Figure 1. “Universal” decay of elastic bulk modulus as function of porosity for a continuous percolation behaviour. The filled circles are measurements on silica while the other data refer to hydroxyapatite (dynamic measurements: diamonds [3] open stars [4] filled stars [5] open circles [6], the line is the self-consistent solution described by Fritsch et al. [7].) The dotted line defines an extrapolated “critical” porosity at $\phi_c = 0.5$.

2. Porous minerals, avalanches, and ferroelasticity

The dramatic mechanical softening due to increasing porosity [8] has indeed been verified in several minerals such as goethite [9], corundum [10], and berlinite [11] which reveal another important property. During the compression of a porous material, one finds a superposition of continuous elastic softening and discontinuous mechanical collapse of the sample. The latter proceeds by avalanches where the collapsed regions penetrate the entire sample [12–15]. Avalanche research parallels research on porous materials, therefore, and is now greatly concentrating on the porous collapse of high-tech materials, such as the highly porous material SiO_2 based vycor [16]. Vycor was found to reproduce many avalanche properties of Californian Earthquakes. Similarly, fracking of oil shales proceeds by avalanches of the porous type [17]. These observations relate the irreversible collapse of porous materials with the same statistical behaviour of reversible domain movements in ferroelastic minerals [18–25]. Some ferroelastic minerals became the archetypal examples for the mechanical and thermal hysteretic behaviour like palmierite $\text{Pb}_3(\text{PO}_4)_2$ and leucite for ferroelastics and PbI_2 for polytypes. This role is comparable with vycor in porous materials for several reasons. Firstly, vycor shows reproducible collapse properties because its porosity is uniform over the entire sample. Secondly, the porosity is ca. 28% which leads to a reduction of the elastic bulk modulus relative to the bulk modulus of the solid SiO_2 matrix to ca. 40% (Figure 1). This reduction is sufficiently large to be beyond the realm of simple perturbation approaches. This softening is in the same order of magnitude as in ferroelastics. It was then discovered that a combination of ferroelasticity and porosity [26] leads to novel structural states under compression and the emergence of polar properties, piezoelectricity

and even ferroelectricity. In that study, the porosity was introduced by cavities which contain surface charges. When a sample is additionally ferroelastic, the cavities nucleate domain walls which connect the cavities. These connections form a complex network of charged walls and cavities and give rise to strong piezoelectricity while the matrix is not piezoelectric at all. Such complex charge patterns are shown in Figure 2. The piezoelectric effect in the domain walls is greatly enhanced by the cavities as seen by the linear component of the strain *versus* electric field correlation in Figure 2e.

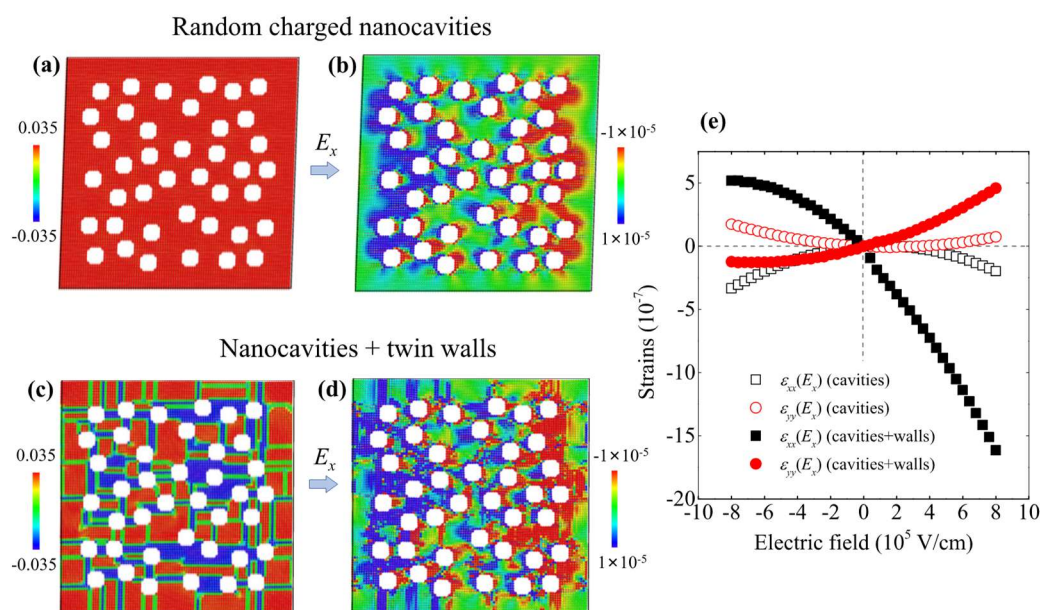


Figure 2. Comparison of electro-mechanical behaviour of a ferroelastic monodomain containing random, negatively charged nanocavities with and without a twinning network. (a) Atomic configuration of a ferroelastic monodomain with periodic distribution of negatively charged nanocavities. The colours are coded according to the atomic-level shear strain (ϵ_{xy}). (b) The response of normal strain under the electrical field E_x . The colours are coded according to the atomic-level normal strain (ϵ_{xx}). (c) A complex twinning network is generated by shearing along x -[10] and y -[01]. The colours are coded according to the atomic-level shear strain (ϵ_{xy}). (d) Response of normal strains under the same electrical field in a twin network with nanocavities. The colours are coded according to the atomic-level normal strain (ϵ_{xx}). (e) The dependence of macroscopic strains $\epsilon_{xx}(E_x)$ and $\epsilon_{yy}(E_x)$ under E_x in two systems. The system containing random negatively charged nanocavities show weak piezoelectricity with $d \sim 8.56 \times 10^{-4}$ pm/V. The piezoelectric effect is greatly enhanced to $d \sim -1.35 \times 10^{-2}$ pm/V when twin walls are injected (reprinted with permission from [26]).

3. Concrete and alloys

Other common porous materials with avalanche processes are concrete mixtures [27] which has been examined particularly extensively using electrical spectroscopy. Here building materials, based

on mineral resources, play a particular role. Much research was related to the breaking of concrete, sandstone etc. Vu et al. [28] showed that on a structural level of porous materials, failure is commonly preceded by an acceleration of the rate of fracturing events, power law distributions of AE energies and durations near failure. This is described by a divergence of the fracturing correlation length and time towards failure. It argues for an interpretation of compressive failure of disordered materials as a critical transition between an intact and a failed state. This emphasises the close connection between these phenomena and ferroelastic phase transitions. Soto-Parra et al. [29] and later Chen et al. [30] showed a similar effect in metallic alloys where mechanical avalanches during compression are found to emit high-frequency acoustic emission (AE) signals. In the case of Ti–Ni alloys, two sequences of AE signals were found in the same sample. The first sequence is mainly generated by detwinning at the early stages of compression while fracture dominates the later stages. Fracture also determines the catastrophic failure (big crash). For samples with high porosity, the AE energies of both sequences display power-law distributions with exponents ϵ similar or equal to 2 (twinning) and 1.7 (fracture). The two power laws confirm that twinning and fracture both lead to avalanche criticality during compression. As twinning precedes fracture, the observation of twinning allows us to predict incipient fracture of the porous shape memory material as an early warning sign (i.e., in bone implants) before the fracture collapse happens.

4. A simple computer model

These observations firmly established acoustic emission studies as a method of choice for the investigation of porous materials. A major step forward was achieved in 2021 when a simple but effective model was proposed by Casals and Salje [31] which reproduces many of the findings in a simple way.

Their model is inspired by a “porous collapse” process where the compression of porous materials generates collapse cascades, leading to power law distributed avalanches. The energy (E), amplitude (A_{max}), and size (S) exponents of these avalanches are derived by computer simulation in two approximations. The average temporal avalanche profile is parabolic [32–34], the scaling between energy and amplitude follows $E \sim A_{max}^2$ [35] and the energy exponent is $\epsilon = 1.33$. Adding a general noise term in a “continuous event model” generates infinite avalanche sequences which allow the evaluation of waiting time distributions and pattern formation. They recover the Omori-law and the same exponents as in the single avalanche model. Spatial correlations are added by stipulating the ratio G/N between growth processes G (linked to a previous event location) and nucleation processes N (with new, randomly chosen nucleation sites). In good approximation, a power law correlation between the energy exponent ϵ and the Hausdorff dimension H_D of the resulting collapse pattern $H_D - 1 \sim \epsilon^{-3}$. The evolving patterns depend strongly on G/N with the distribution of collapse sites equally power law distributed. Its exponent ϵ_{topo} would be linked to the dynamical exponent ϵ if each collapse carried an energy equivalent to the size of the collapse. The model and simulated collapse areas in a porous matrix with triggered individual avalanches are depicted in Figure 3.

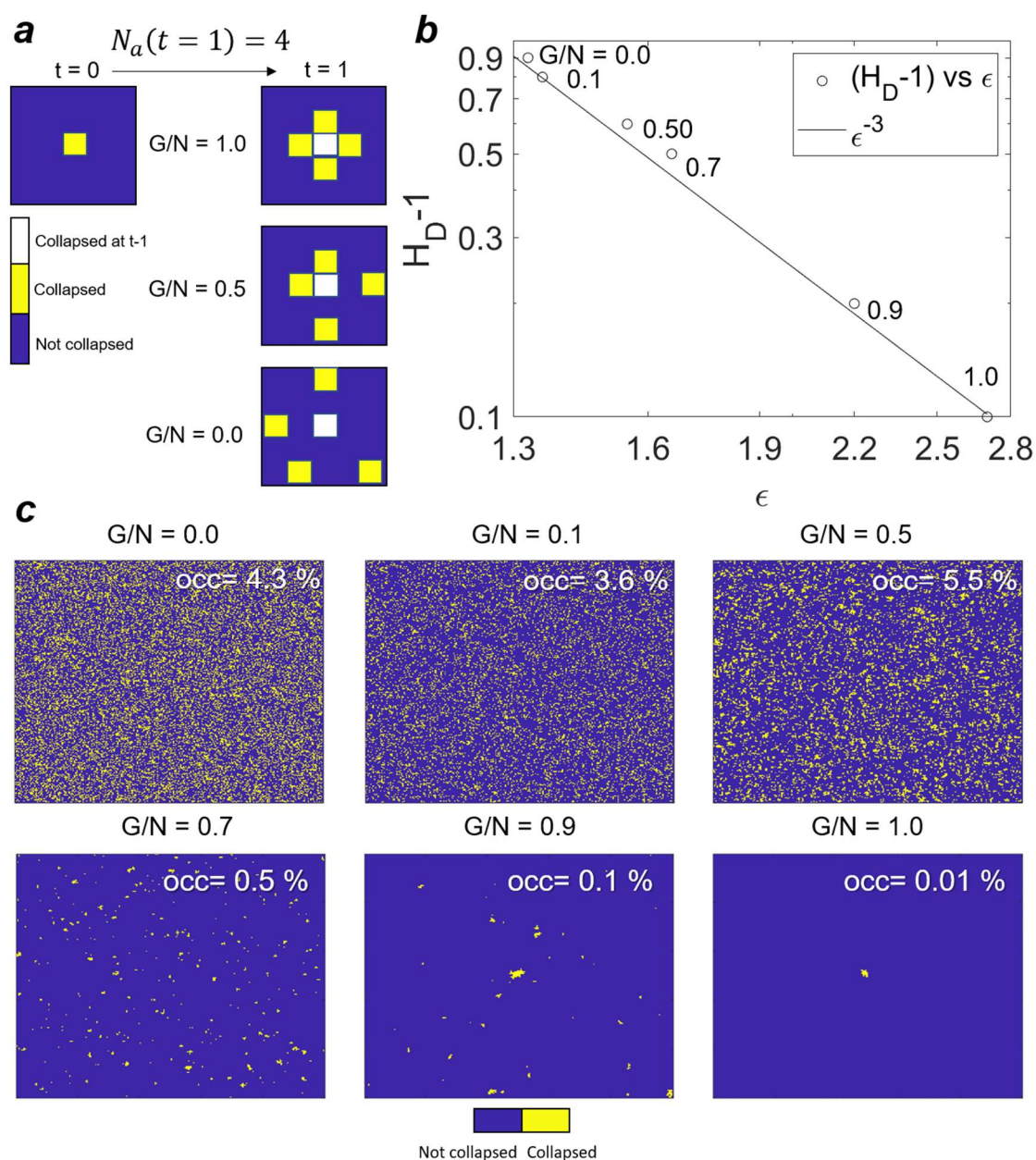


Figure 3. Spatial distribution for the collapse model (single event model). (a) Scheme of the spatial distribution as a function of the G/N percentage. (b) The Hausdorff dimension H_D scales as a function of the energy exponent ϵ for different G/N percentage as $H_D - 1 \sim \epsilon^{-3}$. (c) Examples of the largest event that occurred for different G/N percentages. Images of the frame showing all the collapsed areas after a sequence of single events (after Casals and Salje).

5. Summary

The dynamical behaviour of porous materials under stress is dominated by the formation of collapse avalanches, which form at high stress points and subsequently penetrate the entire sample. They follow simple statistical rules and trace the formation of strain fields. Their internal dynamics

follows approximately the predictions of mean field theory with classic exponents for the energy and size of the avalanches. The collapse patterns can be described by Hausdorff dimensions which are related to the avalanche exponents. Such collapse patterns are common in minerals and high-tech materials alike. Emerging properties due to porosity includes the sudden appearance of piezoelectricity in formally non-piezoelectric materials. The relevant symmetry breaking is not related to the crystal structure but to the formation of nanostructures where the inherent polarity of ferroelastic domain walls combines with wall charges of the embedded cavities.

Acknowledgments

This research was supported by a Grant from EPSRC (No. EP/P024904/1) to E.K.H.S. This project has received funding from the EU's Horizon 2020 programme under the Marie Skłodowska-Curie Grant Agreement No. 861153.

Conflict of interest

All authors declare no conflicts of interest in this paper.

References

1. Salje EKH (2015) Tweed, twins and holes. *Am Mineral* 100: 343–351. <https://doi.org/10.2138/am-2015-5085>
2. Salje EKH, Koppensteiner J, Schranz W, et al. (2010) Elastic instabilities in dry, mesoporous minerals and their relevance to geological applications. *Mineral Mag* 74: 341–350. <https://doi.org/10.1180/minmag.2010.074.2.341>
3. DeWitt G, van Dijk H, Hattu N, et al. (1981) Preparation, microstructure and mechanical properties of dense polycrystalline hydroxyapatite. *J Mater Sci* 16: 1592–1958. <https://doi.org/10.1007/BF00553971>
4. Gilmore RS, Katz JL (1982) Elastic properties of apatites. *J Mater Sci* 17: 1131–1141. <https://doi.org/10.1180/minmag.2010.074.2.341>
5. Liu DMO (1998) Preparation and characterisation of porous hydroxyapatite bioheramic via a slip-casting route. *Ceram Int* 24: 441–446. [https://doi.org/10.1016/S0272-8842\(97\)00033-3](https://doi.org/10.1016/S0272-8842(97)00033-3)
6. Knackstedt MA, Arns CH, Senden TJ, et al. (2006) Structure and properties of clinical coralline implants measured via 3D imaging and analysis. *Biomaterials* 27: 2776–2786. <https://doi.org/10.1016/j.biomaterials.2005.12.016>
7. Fritsch A, Dormieux L, Hellmich C, et al. (2007) Micromechanics of crystal interfaces in polycrystalline solid phases of porous media: fundamentals and application to strength of hydroxy-apatite biomaterials. *J Mater Sci* 42: 8824–8837. <https://doi.org/10.1007/s10853-007-1859-4>
8. Davidsen J, Stanchits S, Dresen G (2007) Scaling and universality in rock fracture. *Phys Rev Lett* 98: 125502. <https://doi.org/10.1103/PhysRevLett.98.125502>

9. Salje EKH, Lampronti GI, Soto-Parra DE, et al. (2013) Noise of collapsing minerals: Predictability of the compressional failure in goethite mines. *Am Min* 98: 609–615. <https://doi.org/10.2138/am.2013.4319>
10. Castillo-Villa PO, Baro J, Planes A, et al. (2013) Crackling noise during failure of alumina under compression: the effect of porosity. *J Phys Condens Matter* 25: 292202. <https://doi.org/10.1088/0953-8984/25/29/292202>
11. Nataf GF, Castillo-Villa PO, Sellappan P, et al. (2014) Predicting failure: acoustic emission of berlinite under compression. *J Phys Condens Matter* 26: 275401. <https://doi.org/10.1088/0953-8984/26/27/275401>
12. Salje EKH, Enrique Soto-Parra E, Planes A, et al. (2011) Failure mechanism in porous materials under compression: crackling noise in mesoporous SiO₂. *Philos Mag Lett* 91: 554–560. <https://doi.org/10.1080/09500839.2011.596491>
13. Nataf G, Castillo-Villa PO, Baro J, et al. (2014) Avalanches in compressed porous SiO₂ materials. *Phys Rev E* 90: 022405. <https://doi.org/10.1103/PhysRevE.90.022405>
14. Alava MJ, Nukala PKVV, Zapperi S (2006) Statistical models of fracture. *Adv Phys* 55: 349–476. <https://doi.org/10.1080/00018730300741518>
15. Hidalgo RC, Grosse CU, Kun F, et al. (2002) Evolution of percolating force chains in compressed granular media. *Phys Rev Lett* 89: 205501. <https://doi.org/10.1103/PhysRevLett.89.205501>
16. Baro J, Corral A, Illa X, et al. (2013) Statistical similarities between the compression of porous material and earthquakes. *Phys Rev Lett* 110: 088702. <https://doi.org/10.1103/PhysRevLett.110.088702>
17. Baro J, Planes A, Salje EKH, et al. (2016) Fracking and labquakes. *Philos Mag* 96: 3686–3696. <https://doi.org/10.1080/14786435.2016.1235288>
18. Bismayer U, Salje E (1981) Ferroelastic phases in Pb₂(PO₄)₂–Pb₃(AsO₄)₂; x-ray and optical experiments. *Acta Cryst A* 37: 145–153. <https://doi.org/10.1107/S0567739481000417>
19. Zapperi S, Ray P, Stanley HE, et al. (1997) First-order transition in the breakdown of disordered media. *Phys Rev Lett* 78: 1408. <https://doi.org/10.1103/PhysRevLett.78.1408>
20. Salje EKH, Wang X, Ding X, et al. (2017) Ultrafast switching in avalanche-driven ferroelectrics by supersonic kink movements. *Adv Funct Mater* 27: 1700367. <https://doi.org/10.1002/adfm.201700367>
21. Zapperi S, Cizeau P, Durin G, et al. (1998) Dynamics of a ferromagnetic domain wall: Avalanches, depinning transition, and the Barkhausen effect. *Phys Rev B* 58: 6353. <https://doi.org/10.1103/PhysRevB.58.6353>
22. Palmer DC, Salje EKH, Schmahl WW (1989) Phase transitions in leucite: X-ray diffraction studies. *Phys Chem Miner* 16: 714–719. <https://doi.org/10.1007/BF00223322>
23. Palosz B, Salje E (1989) Lattice parameters and spontaneous strain in AX₂ polytypes-CdI₂, PbI₂, SnS₂ and SnSe₂. *J Appl Crystallogr* 22: 622–623. <https://doi.org/10.1107/S0021889889006916>
24. Salje EKH, Graeme-Barber A, Carpenter MA, et al. (1993) Lattice parameters, sponmtaneous strain and phase-transitions in Pb₃(PO₄)₂. *Acta crystallogr B* 49: 387–392. <https://doi.org/10.1107/S0108768192008127>

25. Wruck B, Salje EKH, Zhang M, et al. (1994) On the thickness of ferroelastic twin walls in lead phosphate $\text{Pb}_3(\text{PO}_4)_2$ an x-ray-diffraction study. *Phase Transit* 48: 135–148. <https://doi.org/10.1080/01411599408200357>
26. Lu G, Li S, Ding X, et al. (2020) Enhanced piezoelectricity in twinned ferroelastics with nanocavities. *Phys Rev Mater* 4: 074410. <https://doi.org/10.1103/PhysRevMaterials.4.074410>
27. Neithalan N, Weiss J, Olek J (2006) Characterizing enhanced porosity concrete using electrical impedance to predict acoustic and hydraulic performance. *Cem Concr Res* 36: 2074–2085. <https://doi.org/10.1016/j.cemconres.2006.09.001>
28. Vu C-C, Amitrano D, Ple O, et al. (2019) Compressive failure as a critical transition: experimental evidence and mapping onto the universality class of depinning. *Phys Rev Lett* 122: 015502. <https://doi.org/10.1103/PhysRevLett.122.015502>
29. Soto-Parra D, Zhang X, Cao S, et al. (2015) Avalanches in compressed Ti-Ni shape-memory porous alloys: An acoustic emission study. *Phys Rev E* 91: 060401. <https://doi.org/10.1103/PhysRevE.91.060401>
30. Chen Y, Ding XD, Fang DQ, et al. (2019) Acoustic emission from porous collapse and moving dislocations in granular Mg-Ho alloys under compression and tension. *Sci Rep* 9: 1330. <https://doi.org/10.1038/s41598-018-37604-5>
31. Casals B, Salje EKH (2021) Energy exponents of avalanches and Hausdorff dimensions of collapse patterns. *Phys Rev E* 104: 054138. <https://doi.org/10.1103/PhysRevE.104.054138>
32. Bingham NS, Rooke S, Park J, et al. (2021) Experimental realization of the 1D random field Ising model. *Phys Rev Lett* 127: 207203. <https://doi.org/10.1103/PhysRevLett.127.207203>
33. He X, Ding X, Sun J, et al. (2016) Parabolic temporal profiles of non-spanning avalanches and their importance for ferroic switching. *Appl Phys Lett* 108: 072904. <https://doi.org/10.1063/1.4942387>
34. McFaul LW, Wright WJ, Sickle J, et al. (2019) Force oscillations distort avalanche shapes. *Mater Res Lett* 7 496–502. <https://doi.org/10.1080/21663831.2019.1659437>
35. Casals B, Dahmen KA, Gou B, et al. (2021) The duration-energy-size enigma for acoustic emission. *Sci Rep* 11: 5590. <https://doi.org/10.1038/s41598-021-84688-7>



AIMS Press

© 2022 the Author(s), licensee AIMS Press. This is an open access article distributed under the terms of the Creative Commons Attribution License (<http://creativecommons.org/licenses/by/4.0>)